Hindawi Publishing Corporation
Journal of Nanomaterials
Volume 2013, Article ID 131537, 6 pages
http://dx.doi.org/10.1155/2013/131537

Research Article

Thermoelectric Properties of Al-Doped Mesoporous ZnO Thin Films

Min-Hee Hong,[1] Chang-Sun Park,[1] Won-Seon Seo,[2] Young Soo Lim,[2] Jung-Kun Lee,[3] and Hyung-Ho Park[1]

[1] *Department of Materials Science and Engineering, Yonsei University, Seoul 120-749, Republic of Korea*
[2] *Korea Institute of Ceramic Engineering and Technology, Seoul 153-801, Republic of Korea*
[3] *Department of Mechanical Engineering and Materials Science, University of Pittsburgh, Pittsburgh, PA 15261, USA*

Correspondence should be addressed to Hyung-Ho Park; hhpark@yonsei.ac.kr

Received 7 June 2013; Accepted 25 August 2013

Academic Editor: Chan Park

Al-doped mesoporous ZnO thin films were synthesized by a sol-gel process and an evaporation-induced self-assembly process. In this work, the effects of Al doping concentration on the electrical conductivity and characterization of mesoporous ZnO thin films were investigated. By changing the Al doping concentration, ZnO grain growth is inhibited, and the mesoporous structure of ZnO is maintained during a relatively high temperature annealing process. The porosity of Al-doped mesoporous ZnO thin films increased slightly with increasing Al doping concentration. Finally, as electrical conductivity was increased as electrons were freed and pore structure was maintained by inhibiting grain growth, the thermoelectric property was enhanced with increasing Al concentration.

1. Introduction

Development of alternative energy is very important because fossil fuels are being rapidly depleted. Thermoelectricity is a very important green energy conversion technique, as waste heat could be used. When materials have a temperature gradient, electric current is generated in the materials. To maintain a high thermoelectric property, factors of Seebeck coefficient, electrical conductivity, and thermal conductivity need to be controlled individually. However, among thermoelectric factors, electrical conductivity and thermal conductivity have a proportional relationship. To overcome this problem, studies on structure change have been performed, including studies on nanostructures, nanowires, and superlattices [1]. Of the structures studied, mesoporous structures could be adapted to thermoelectrics because mesoporous structures have low thermal conductivity. Mesoporous materials have pores that range between 2 and 50 nm [2]. Because of their pore structure, mesoporous structures have properties such as a high specific surface area, low dielectric constant, and low thermal conductivity. In the evaporation-induced self-assembly (EISA) process, a micelle structure is formed and an ordered pore structure is synthesized after the annealing process. When the surfactant concentration exceeds the critical micelle concentration, the EISA process progresses. Good thermoelectric materials have high Seebeck coefficient and electrical conductivity and low thermal conductivity. The order of the pore structure is very important to controlling the electrical conductivity and the thermal conductivity individually because the inelastic mean free path of electrons and phonons is different. This difference is generally referred to as the phonon-glass electron crystal (PGEC) effect. Because the inelastic mean free path of an electron is longer than that of a phonon, phonons are scattered effectively in ordered mesoporous structures [3, 4]. In order to maximize the PGEC effect, a doping source with an inhibited grain growth property is used because its ordered pore structure is less prone to collapse.

Zinc oxide (ZnO) is an important n-type wide band gap semiconductor material used in various applications such as photovoltaic devices [5], gas sensors [6], and solar cells [7]. By using physical vapor deposition, chemical vapor deposition, and the sol-gel process [8–10], ZnO thin films can be easily synthesized. In this work, the sol-gel process was

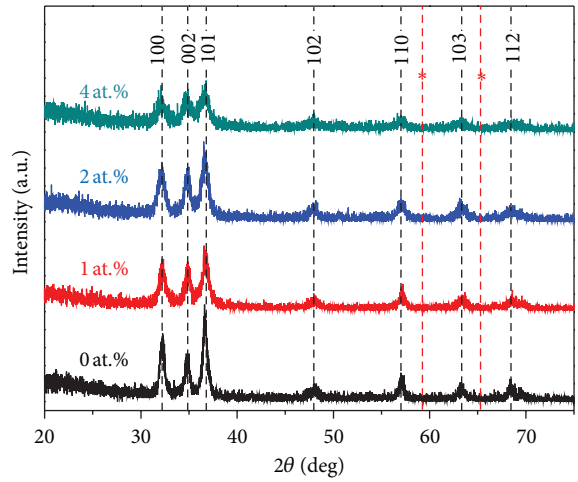

Figure 1: Wide-angle XRD patterns of Al-doped mesoporous ZnO thin films with various Al doping concentrations (∗ represents a typical diffraction peak position of $ZnAl_2O_4$ at high angle 2 theta region).

selected to adapt the EISA process. ZnO could be doped with various group III materials such as In, Ga, and Al. Among the many doping materials, Al-doped ZnO thin films are most important for this application. Because Al-doped ZnO thin films have high thermal stability and are inexpensive, they have been studied as possible next-generation materials to replace indium tin oxides [11]. In this work, Al was doped to increase its thermoelectric properties. When Al was doped in ZnO, the electrical conductivity was increased [12]. Moreover, the grain growth of ZnO was effectively inhibited [13]. In Al doping, Al ions are substituted at Zn ion sites. In this process, the hexagonal wurtzite structure is distorted because of the difference in the radius of Al^{3+} (0.054 nm) and Zn^{2+} (0.074 nm). Finally, the crystalline structure deteriorates because when stress forms in thin films, the grain growth of the hexagonal wurtzite structure is inhibited. In a mesoporous structure, high temperature stability is essential to maintaining an ordered pore structure. An Al-doped mesoporous ZnO thin film could have good thermoelectric properties because it has a high electrical conductivity and high temperature stability due to inhibited grain growth. In this paper, the effects of Al concentration on the pore arrangement in mesoporous ZnO thin films and on the crystallization, pore structure, porosity, and thermoelectric property of the film were analyzed.

2. Experimental Procedure

Al-doped mesoporous ZnO thin films were prepared on SiO_2/Si substrates by sol-gel and spin coating processes. Zinc acetate dihydrate [$Zn(CH_3COO)_2{\cdot}H_2O$], n-propanol, Brij-76 ($C_{58}H_{118}O_{21}$, Aldrich, MW 711), aluminum nitrate nonahydrate [$Al(NO_3){\cdot}9H_2O$], and monoethanolamine (MEA) were used as Zn precursor, solvent, surfactant, dopant source, and complex agent, respectively. The molar ratios of MEA/Zn precursor and surfactant/Zn precursor were fixed at 1 and 0.05 in this work. The molar ratio of zinc acetate dihydrate : Brij-76 : MEA : n-propanol was 1 : 0.05 : 1 : 34.5. The atomic ratio of Al precursor and Zn precursor was changed from 0 at.% to 4 at.%. The precursor solutions were spin coated onto SiO_2/Si substrate. Solvent was evaporated during the spin coating process. Then, the EISA process was started in the thin films and a micelle structure was synthesized. As-prepared thin films were preheated at 300°C for 10 min to remove residual organics. After preheating, Al-doped mesoporous ZnO thin films were annealed at 650°C for 4 h. To investigate the resulting ordered pore structure, small-angle X-ray diffraction (SAXRD) was performed with Cu Kα radiation (λ = 1.5418 Å) at angles of 1° to 5°. Grazing incidence small-angle X-ray scattering (GISAXS) at the 3C beam line (λ = 1.54 Å and $\Delta\lambda/\lambda = 5 \times 10^{-4}$) of the Pohang Light Source (PLS) in Korea was also used to investigate the pore arrangement of the thin film [14]. Porosity was measured with an ellipsometer (Gatan L117C, 632.8 nm He-Ne laser) and calculated using the Lorentz-Lorenz equation [15]. The thermoelectric properties of Al-doped ZnO thin films were measured by detecting the Seebeck voltage with SEEPEL thermoelectric properties measurement system (TEP 850) and the temperature difference from 323 K to 478 K at intervals of 50 K in flowing helium gas atmosphere.

3. Results and Discussion

Regardless of Al concentration, all mesoporous ZnO thin films have a hexagonal wurtzite structure. Diffraction peaks at 31.8°, 33.4°, and 36.2° were indexed as 100, 002, and 101, respectively. A distinguished diffraction peak from $ZnAl_2O_4$ secondary phase was not observed at around 59.3° and 65.2° of 2 theta (JCPDS card no. 82-1043), although a formation of $ZnAl_2O_4$ has been reported with doping of Al more than solubility limit in ZnO structure, for example, around 3 at.% of Al [16]. However, all samples had the same crystal phase and hexagonal wurtzite structure, peak intensity decreased with increasing Al concentration, as shown in Figure 1. Because of the smaller radius of Al^{3+} (0.054 nm) compared with that of Zn^{2+} (0.074 nm), crystallization of ZnO was

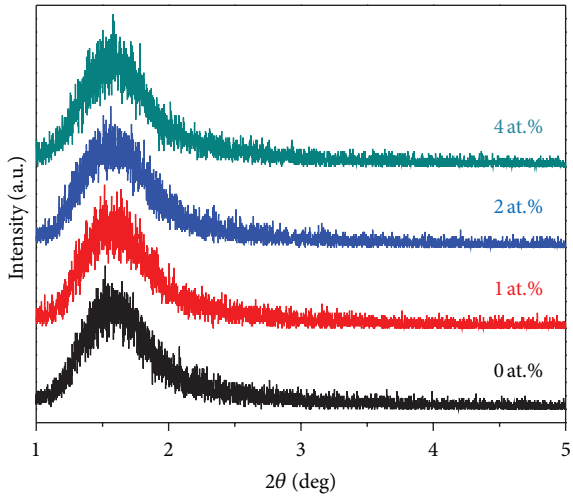

Figure 2: Small-angle XRD patterns of Al-doped mesoporous ZnO thin films with various Al doping concentrations.

inhibited by Al doping. Furthermore undetected $ZnAl_2O_4$ secondary phase from the XRD measurement might act a grain boundary pinning site, that is, grain growth inhibitor. Based on this result, the grain growth of ZnO was inhibited with increasing Al concentration. The Al doping process enhances electrical conductivity via n-type dopant and pore structure reinforcement in a mesoporous ZnO structure, which acts as a grain growth inhibitor during the high-temperature annealing process. In general, the crystallization of ZnO is started at low temperatures in the sol-gel process [12]. Because of grain growth in skeleton-structured ZnO, the pore structure of mesoporous ZnO could collapse easily. However, with Al doping, grain growth could be inhibited effectively and pore structure could be maintained compared with mesoporous pure ZnO. To investigate the relationship between crystallization and an ordered pore structure, SAXRD was used in the range of 1° to 5°. As shown in Figure 2, broad SAXRD peaks could be observed at around 1.61° of 2θ in all samples. All samples showed broad diffraction peaks, which suggests that a partially ordered pore structure is present in the thin films [17]. Because of the high-temperature annealing, the ordered pore structure collapsed and was replaced with a partially ordered pore structure, as shown at Figure 2. The partially ordered structure showed a broad peak at around 1.61°. Regardless of Al concentration, peak intensity was also very similar to pure mesoporous ZnO and Al-doped samples. All samples showed an inter-pore distance of 5.47 nm. The hexagonal wurtzite structure is inhibited by Al doping [18] so that the pore structure is affected. GISAXS analysis was used to analyze the pore structure in more detail. When an X-ray is scattered at the surface of a sample at a low grazing incidence, an X-ray is emitted due to changes in the surface density. Because the emitted X-ray strikes the two-dimensional detector in the horizontal and vertical dimensions, the pore structure can be analyzed in detail [19]. As shown in Figure 3, the GISAXS pattern was enlarged in the horizontal directions with increasing Al concentration. In GISAXS, enlargement in the scattering pattern in the horizontal or vertical directions indicates an ordered pore structure in the horizontal or vertical directions in the thin film. In the case of pure mesoporous ZnO thin films, a partially ordered pore structure pattern and scattering pattern were observed together, meaning that the ordered pore structure exists partially in the horizontal and vertical direction in thin films. However, as the Al doping concentration increased, the partially ordered pore structure scattering pattern in the horizontal direction became more apparent. As shown in Figure 3, the ordering of the pore arrangement was enhanced by increased Al concentration. Based on this result, the partially ordered pore structures of Al-doped mesoporous ZnO thin films were maintained because the grain growth of hexagonal wurtzite was effectively inhibited.

The grain growth of ZnO was prevented by Al doping. The pore arrangement also changed, as shown in Figure 3. This change in the pore arrangement could affect porosity. The variation in porosity with Al doping in the mesoporous structure was calculated using the Lorentz-Lorenz equation.

Consider

$$1 - F_P = \frac{\left(n_f^2 - 1\right) / \left(n_f^2 + 2\right)}{\left(n_a^2 - 1\right) / \left(n_a^2 + 2\right)}, \quad (1)$$

where F_p is the pore volume fraction, n_f is the refractive index of the film, and n_a is the refractive index of air. Figure 4 shows the variation in the porosity of Al-doped mesoporous ZnO thin films. As Al concentration changed, porosity also changed slightly from 34% to 39%. Although the porosity was decreased at 4 at.% Al doping, the porosity tends to increase slightly with Al doping concentration. Because the grain growth of ZnO was inhibited, the pore structure collapsed less at the same annealing temperature, and the porosity increased slightly. Based on this result, we conclude that about 5% of porosity could be affected by grain growth.

Figure 5 shows the change in the Seebeck coefficient at various Al doping concentrations. All Seebeck coefficient values are in the negative range because ZnO is n-type. When the Al concentration increases to 2 at.%, the Seebeck coefficient is decreased. Because the number of free electrons increases, the carrier concentration in the ZnO thin film increases. In general, the Seebeck coefficient and carrier concentration are inversely related. The Seebeck coefficient value decreases as the Al doping process progresses. When Al is doped at 0 at.% in mesoporous ZnO thin films, the highest Seebeck coefficient at 383 K is −75.72 μV/K. Although the Seebeck coefficient is at a minimum when the Al concentration is 2 at.% with a value of −63.58 μV/K at 383 K, the decrease in the Seebeck coefficient was not large. The electrical conductivity was higher due to the increase in free electrons. The thermal conductivity declined because the ordered pore structure was maintained better than in pure mesoporous ZnO.

Electrical conductivity at various Al concentrations is shown in Figure 6. The electrical conductivity increased with increased Al concentration. The average electrical conductivity values of 0, 1, 2, and 4 at.% Al-doped mesoporous ZnO thin

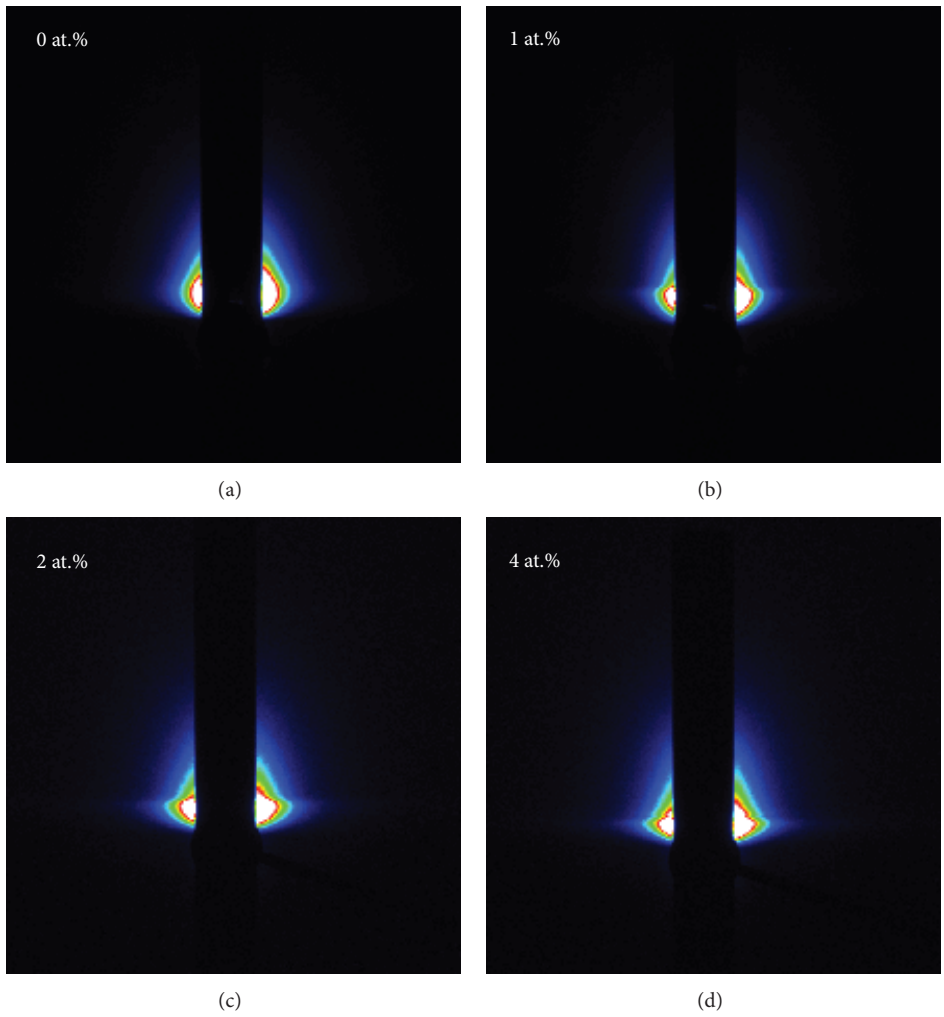

Figure 3: GISAXS patterns of Al-doped mesoporous ZnO thin films with various Al doping concentrations.

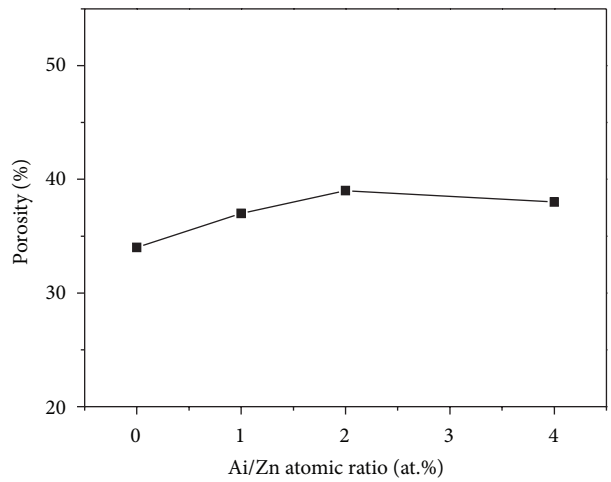

Figure 4: Porosity change in Al-doped mesoporous ZnO thin films with various Al doping concentrations.

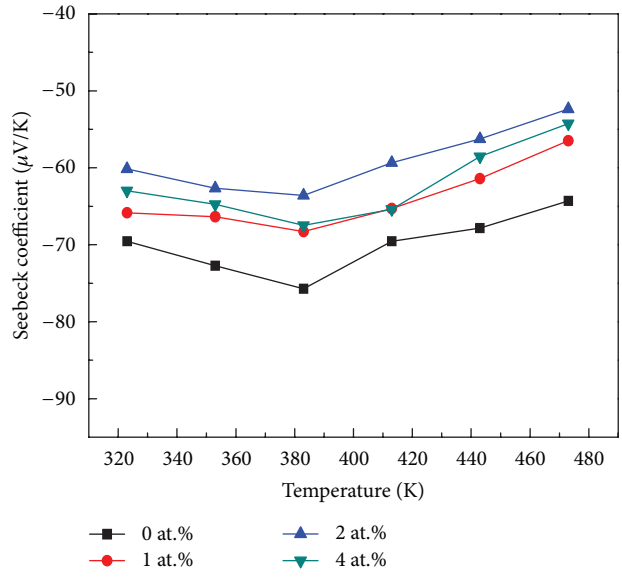

Figure 5: Seebeck coefficients of Al-doped mesoporous ZnO thin films with various Al doping concentrations.

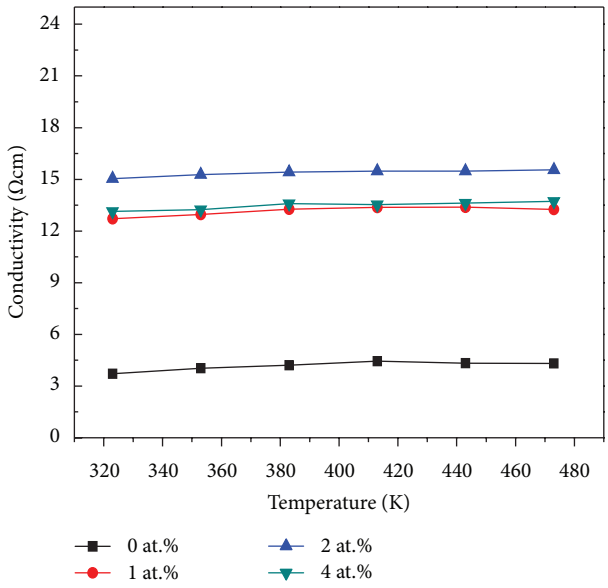

Figure 6: Electrical conductivity changes in Al-doped mesoporous ZnO thin films with various Al doping concentrations.

films were 4.17, 13.15, 15.37, and 13.47/Ωcm. When compared with pure mesoporous ZnO, the electrical conductivities increased by about 3.5 times. Mesoporous ZnO thin films with 2 at.% Al doping showed the highest electrical conductivity. However, in the case of 4 at.% Al doping, the electrical conductivity decreased slightly due to increased scattering at the center due to excess Al doping [20]. Comparing the Seebeck coefficient and electrical conductivity, it can be seen that Al doping in mesoporous ZnO enhanced the thermoelectric properties. Although the Seebeck coefficient decreased, the increase in electrical conductivity is very high, and thus the thermoelectric properties increased. For example, when Al is doped in mesoporous ZnO, the Seebeck coefficient decreases by about 20%. However, electrical conductivity increases by about 3.5 times. For this reason, the power factor ($S^2\sigma$) increased by a factor of 3. When Al is used to dope ZnO, the thermal conductivity of the electron term is increased. However, the contribution of the electron in thermal conductivity was very small [21]. The thermal conductivity of the phonon might have decreased, because the grain growth in ZnO is inhibited, which maximizes the PGEC effect. Finally, the thermoelectric properties of mesoporous ZnO thin films could be increased with an Al doping process.

4. Conclusion

In this work, Al-doped mesoporous ZnO thin film was synthesized. The Al doping concentration was varied from 0 at.% to 4 at.% to investigate the crystal structure and thermoelectric properties. The phase formation of ZnO with hexagonal wurtzite structure and the grain growth were inhibited from an increased doping concentration of Al. Therefore, a partially ordered pore structure could be maintained after anneal by doping with Al. Although the Seebeck coefficient was decreased with increasing Al concentration, the decrease in the Seebeck coefficient was relatively small and the increase in the electrical conductivity was large. The thermoelectric properties were enhanced by a factor of 3 as the Al doping concentration increased. As a result, the mesoporous ZnO thin film showed better thermoelectric properties after Al doping.

Acknowledgments

This research was supported by a Grant from the Fundamental R&D Program (Grant no. K0006007) for the Core Technology of Materials funded by the Ministry of Knowledge Economy, Republic of Korea. This work was also supported by the National Research Foundation of Korea (NRF) Grant funded by the Korean government (MEST) (no. 2012R1A2A2A01011014). Experiments at PLS were supported in part by MEST and POSTECH.

References

[1] M. S. Dresselhaus and L. D. Hicks, "Effect of quantum-well structures on the thermoelectric figure of merit," *Physical Review B*, vol. 47, no. 19, pp. 12727–12731, 1993.

[2] G. J. Soler-Illia, C. Sanchez, B. Lebeau, and J. Patarin, "Chemical strategies to design textured materials: from microporous and mesoporous oxides to nanonetworks and hierarchical structures," *Chemical Reviews*, vol. 102, no. 11, pp. 4093–4138, 2002.

[3] D. M. Rowe, *CRC Handbook of Thermoelectrics*, CRC Press, New York, NY, USA, 1995.

[4] G. J. Snyder, M. Christensen, E. Nishibori, T. Caillat, and B. B. Iversen, "Disordered zinc in Zn_4Sb_3 with phonon-glass and electron-crystal thermoelectric properties," *Nature Materials*, vol. 3, no. 7, pp. 458–463, 2004.

[5] Q. Zhang, C. S. Dandeneau, X. Zhou, and C. Cao, "ZnO nanostructures for dye-sensitized solar cells," *Advanced Materials*, vol. 21, no. 41, pp. 4087–4108, 2009.

[6] H.-W. Ra, K.-S. Choi, J.-H. Kim, Y.-B. Hahn, and Y.-H. Im, "Fabrication of ZnO nanowires using nanoscale spacer lithography for gas sensors," *Small*, vol. 4, no. 8, pp. 1105–1109, 2008.

[7] Q. Zhang, C. S. Dandeneau, X. Zhou, and C. Cao, "ZnO nanostructures for dye-sensitized solar cells," *Advanced Materials*, vol. 21, no. 41, pp. 4087–4108, 2009.

[8] Y. Natsume and H. Sakata, "Zinc oxide films prepared by sol-gel spin-coating," *Thin Solid Films*, vol. 372, no. 1-2, pp. 30–36, 2000.

[9] M. Smirnov, C. Baban, and G. I. Rusu, "Structural and optical characteristics of spin-coated ZnO thin films," *Applied Surface Science*, vol. 256, no. 8, pp. 2405–2408, 2010.

[10] T. Sahoo, M. Kim, M.-H. Lee et al., "Nanocrystalline ZnO thin films by spin coating-pyrolysis method," *Journal of Alloys and Compounds*, vol. 491, no. 1-2, pp. 308–313, 2010.

[11] S. Fujihara, C. Sasaki, and T. Kimura, "Crystallization behavior and origin of c-axis orientation in sol-gel-derived ZnO:Li thin films on glass substrates," *Applied Surface Science*, vol. 180, no. 3-4, pp. 341–350, 2001.

[12] Z.-Q. Xu, H. Deng, Y. Li, and H. Cheng, "Al-doping effects on structure, electrical and optical properties of c-axis-orientated ZnO:Al thin films," *Materials Science in Semiconductor Processing*, vol. 9, no. 1–3, pp. 132–135, 2006.

[13] S. Mridha and D. Basak, "Aluminium doped ZnO films: electrical, optical and photoresponse studies," *Journal of Physics D*, vol. 40, no. 22, pp. 6902–6907, 2007.

[14] B. Lee, I. Park, J. Yoon et al., "Structural analysis of block copolymer thin films with grazing incidence small-angle X-ray scattering," *Macromolecules*, vol. 38, no. 10, pp. 4311–4323, 2005.

[15] M. R. Baklanov, K. P. Mogilnikov, V. G. Polovinkin, and F. N. Dultsev, "Determination of pore size distribution in thin films by ellipsometric porosimetry," *Journal of Vacuum Science and Technology B*, vol. 18, no. 3, pp. 1385–1391, 2000.

[16] M. H. Yoon, S. H. Lee, H. L. Park, H. K. Kim, and M. S. Jang, "Solid solubility limits of Ga and Al in ZnO," *Journal of Materials Science Letters*, vol. 21, no. 21, pp. 1703–1704, 2002.

[17] D. Grosso, G. J. Soler-Illia, F. Babonneau et al., "Highly organized mesoporous titania thin films showing mono-oriented 2D hexagonal channels," *Advanced Materials*, vol. 13, no. 14, pp. 1085–1090, 2001.

[18] J.-H. Lee and B.-O. Park, "Characteristics of Al-doped ZnO thin films obtained by ultrasonic spray pyrolysis: effects of Al doping and an annealing treatment," *Materials Science and Engineering B*, vol. 106, no. 3, pp. 242–245, 2004.

[19] D. A. Doshi, A. Gibaud, V. Goletto et al., "Peering into the self-assembly of surfactant templated thin-film silica mesophases," *Journal of the American Chemical Society*, vol. 125, no. 38, pp. 11646–11655, 2003.

[20] H.-M. Zhou, D.-Q. Yi, Z.-M. Yu, L.-R. Xiao, and J. Li, "Preparation of aluminum doped zinc oxide films and the study of their microstructure, electrical and optical properties," *Thin Solid Films*, vol. 515, no. 17, pp. 6909–6914, 2007.

[21] S. O. Kasap, *Principles of Electronic Materials and Devices*, McGraw-Hill, New York, NY, USA, 3rd edition, 2006.